

## A new formula of loess earth pressures based on the joint strength theory

P. Sun<sup>1</sup>, R.-J. Li<sup>2,\*</sup>, O. Igwe<sup>3</sup>, H. Luo<sup>2</sup>

<sup>1</sup> Institute of Geomechanics, Chinese Academy of Geological Sciences, Beijing 100081, China

<sup>2</sup> Shaanxi provincial key laboratory of loess mechanics and engineering, Xi'an University of Technology, Xi'an 710048, China

<sup>3</sup> Department of Geology, University of Nigeria, Nsukka, Nigeria

Received May 25, 2017; Revised July 20, 2017

Because the effect of tensile strength on the calculation of the earth pressure of loess is worthy of further evaluation, based on the joint strength theory that fully considers tensile and shear properties of loess, this paper first analyzes active and passive limit stress equilibrium, then derives new calculation formulae for active and passive earth pressures, and finally verifies these new formulae and compares them with Rankine's classical formulae for active and passive earth pressures. The results show that the active earth pressure of loess based on the joint strength theory is larger than the Rankine's active earth pressure; the passive earth pressure of loess based on the joint strength theory is smaller than the Rankine's passive earth pressure.

**Keywords:** loess, tensile strength, joint strength formula, active earth pressure, passive earth pressure

### INTRODUCTION

Classical earth pressure theories derived from the Mohr-Coulomb strength theory, mainly include Rankine's earth pressure theory and Coulomb's earth pressure theory [1].

The concept of earth pressure calculation was put forward in 1773. Coulomb's earth pressure theory [2] and Rankine's earth pressure theory [3] are two classical earth pressure theories proposed in 1776 and 1857 respectively. These studies have laid the preliminary foundation for the research on earth pressures.

Xie et al. [4] and Gao et al. [5] derived formulae to calculate active earth pressures and passive earth pressures. Zhang et al. [6] obtained formulae to calculate active and passive earth pressures. The above studies promoted the calculation of earth pressures on the retaining wall.

To expand the research fields of earth pressures, Nakai et al. [7] introduced the FEM into the calculation of earth pressures on the retaining wall. Zhu et al. [8] set up unified expressions of earth pressures on the inclined retaining wall. Hu et al. [9] studied active earth pressures on a retaining wall in a non-limit state via the thin-layer element method. Zhao et al. [10] established a unified solution to Coulomb's active earth pressures of unsaturated earth. And Ma et al. [11] introduced the concept of structurality of loess to the calculation of earth pressures. The above studies have promoted the development of earth pressure. However, all these studies failed to discuss or evaluate the tensile

strength of structural loess.

In order to consider the tensile strength of structural loess reasonably, Li et al. [12-14] introduced structural parameters into the joint strength theory for structural loess, and put forward a simplified hyperbolic strength formula for structural loess. In addition, based on the hyperbolic strength formula for structural loess, Song et al. [15] introduced structural parameters to the hyperbolic strength formula for structural loess. The above results have fully considered the tensile strength and the shear strength of structural loess.

Therefore, based on the joint strength theory that fully considers tensile and shear properties of loess and through analyzing active and passive limit stress equilibrium, new calculation formulae for active and passive earth pressures will be derived, verified and compared with Rankine's classical formulae in the present study.

### METHODS

#### *The joint strength theory*

To evaluate the tensile strength effect of structural loess reasonably, the curvilinear relation between tensile strength  $\sigma_t$  and cohesion force  $c$  obtained by tests, as shown in Fig.1. Formula (1) is the fitting formula.

$$\sigma_t = 10^{-6} c^3 - 0.0011c^2 + 0.7081c - 1.8913 \quad (1)$$

Via tensile tests and triaxial shear tests, Li et al. [12] obtained strength failure stress circles as shown in Fig.2. Via analyzing Fig.2, the tensile strength values based on the reverse extension lines of Mohr-Coulomb strength lines are 2~3 times significantly higher than the corresponding actual test values.

\* To whom all correspondence should be sent:  
E-mail: lirongjian@xaut.edu.cn

Results indicate that the Mohr-Coulomb failure criterion overestimate the tensile strength of loess.

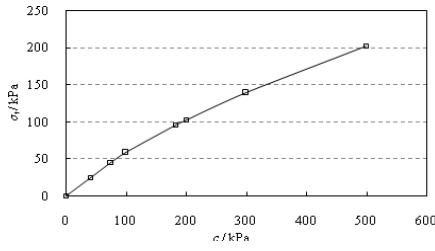


**Fig. 1.** The correlation between the tensile strength and the cohesive force of structural loess

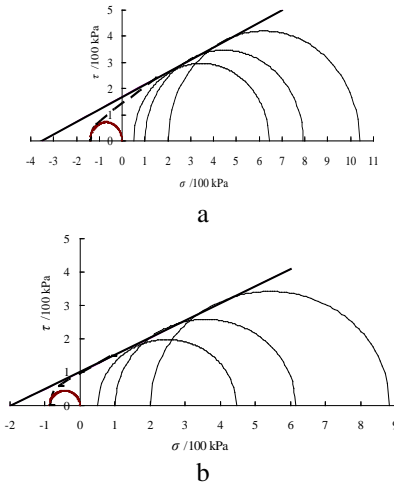


**Fig.2** The strength failure lines based on their tensile and shear properties: a) Intact loess; b) Remolded loess.

In Fig.2, Mohr-Coulomb strength lines in the tension-shear region are represented by smooth curves. Apparently, one strength line can be obtained after curve-fitting with a smooth curve used in the tension-shear zone and pressure-shear zone respectively. As a result, the strength line can reflect the tension-shear and pressure-shear failure.

In plane  $\sigma$ - $\tau$ , the joint strength formula can be shown as follow:

$$\tau^2 = (c + \sigma \tan \varphi)^2 - (c + \sigma_t \tan \varphi)^2 \quad (2)$$

Among them,  $\varphi$  is the internal friction angle of the backfill behind the wall.

#### Derivation premise and hypothesis on loess earth pressures based on the joint strength theory

The basic assumption is adopted in the Rankine's earth pressure theory. As shown in Fig.3,  $\sigma_h$  stands for the horizontal stress, and  $\sigma_v$  stands for the vertical stress.

For the convenient description, the joint strength line is divided into three sections: section I indicates the strength line with the horizontal stress in the tensile-shear region, section II indicates the strength

curve with the horizontal stress in the pressure-shear region, and section III indicates the strength straight line with the horizontal stress in the pressure-shear region, as shown in Fig.4.

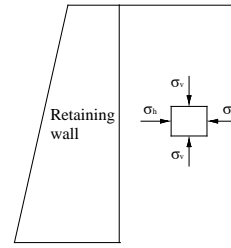


**Fig. 3** The stress state of soil in slope.

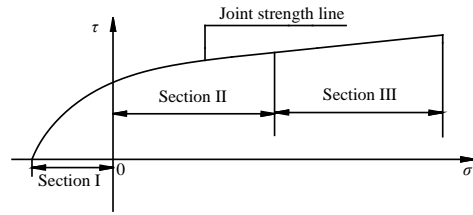


**Fig. 4.** The segmentation of a joint strength line.

## RESULTS

### Derivation and analysis of active earth pressures of loess based on the joint strength theory

#### Analysis of limit equilibrium state in active earth pressure

When the horizontal force  $\sigma_h$  decreases to a certain extent, the Mohr's stress circle is right tangent to the joint strength line. At this point, the horizontal force  $\sigma_h$  is the active earth pressure  $p_a$ .

The active limit equilibrium state of soil can be analyzed in three cases (Fig.4). In the first case, the horizontal stress decreases to the extent that the Mohr's circle is tangent to section III; in the second case, the horizontal stress decreases to the extent that the Mohr's circle is tangent to section II; and in the third case, the horizontal stress decreases to the extent that the Mohr's circle is tangent to section I. When the soil is in a state corresponding to the first case:

$$p_a = \gamma z \tan^2 \left( 45^\circ - \frac{\varphi}{2} \right) - 2c \tan \left( 45^\circ - \frac{\varphi}{2} \right) \quad (3)$$

When the soil is in a state corresponding to the second or third case, active earth pressures on the retaining wall can be derived based on the joint strength.

#### (2) Derivation of new loess active earth pressure

When the Mohr's stress circle is in an active limit equilibrium state (as shown in Fig.5). Assume that point G is the tangent point, point E is the center of

the Mohr's stress circle, and line segment GF is perpendicular to axis  $\sigma$  with point F as the pedal point.

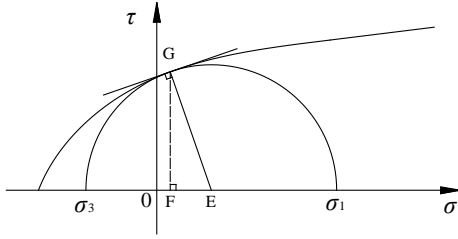


Fig. 5. The active limit equilibrium state

According to formula(2), the ordinate of point G can be obtained. So G (  $\sigma_G$  ,  $\sqrt{(c + \sigma_G \tan \varphi)^2 - (c + \sigma_i \tan \varphi)^2}$  ). The slope  $k_t$  of the tangent point G can be calculated as:

$$k_t = \frac{d\tau}{d\sigma} = \frac{(c + \sigma_G \tan \varphi) \tan \varphi}{\sqrt{(c + \sigma_G \tan \varphi)^2 - (c + \sigma_i \tan \varphi)^2}} \quad (4)$$

Accordingly, the equation for the normal line at point G can be calculated as:

$$\tau - \tau_G = -\frac{1}{k_t}(\sigma - \sigma_G) \quad (5)$$

Based on formula(5) and equation  $\tau=0$ , the abscissas of E can be acquired as:

$$\sigma_E = \frac{1}{\cos^2 \varphi} \sigma_G + c \tan \varphi \quad (6)$$

Therefore, center point E (  $\frac{1}{\cos^2 \varphi} \sigma_G + c \tan \varphi$  , 0).

In  $\Delta GFE$ ,  $|GF| = \tau_G$  and  $|FE| = k_t \tau_G$ . The radius of the Mohr's stress circle can be expressed:

$$|EG| = \sqrt{(k_t \tau_G)^2 + \tau_G^2} \quad (7)$$

The equation for the corresponding Mohr's stress circle can be determined as:

$$\left[ \sigma - \left( \frac{1}{\cos^2 \varphi} \sigma_G + c \tan \varphi \right) \right]^2 + \tau^2 = \tau_G^2 (1 + k_t^2) \quad (8)$$

When  $\tau=0$  in equation(8), the major principal stress ( $\sigma_1$ ) and the minor principal stress ( $\sigma_3$ ) can be calculated respectively as:

$$\sigma_1 = \frac{1}{\cos^2 \varphi} \sigma_G + c \tan \varphi + \sqrt{\tau_G^2 + \tau_G^2 k_t^2} \quad (9)$$

$$\sigma_3 = \frac{1}{\cos^2 \varphi} \sigma_G + c \tan \varphi - \sqrt{\tau_G^2 + \tau_G^2 k_t^2} \quad (10)$$

Put formula (4) and  $\tau_G$  into formula(9) and formula(10), then:

$$\sigma_1 = \frac{1}{\cos^2 \varphi} \sigma_G + c \tan \varphi + \sqrt{(c + \sigma_G \tan \varphi)^2 \cdot \frac{1}{\cos^2 \varphi} - (c + \sigma_i \tan \varphi)^2} \quad (11)$$

$$\sigma_3 = \frac{1}{\cos^2 \varphi} \sigma_G + c \tan \varphi - \sqrt{(c + \sigma_G \tan \varphi)^2 \cdot \frac{1}{\cos^2 \varphi} - (c + \sigma_i \tan \varphi)^2} \quad (12)$$

According to formula(11), an inverse solution can be made as:

$$\sigma_G = -\sqrt{\sin^2 \varphi \cdot \sigma_i^2 + 2c \sin \varphi \cdot \cos \varphi \cdot \sigma_i - \cos^2 \varphi (\sigma_i^2 \tan^2 \varphi + 2c \cdot \sigma_i \tan \varphi)} + \sigma_i \quad (13)$$

To simplify formulae, let:

$$\begin{cases} A = -\cos^2 \varphi (\sigma_i^2 \tan^2 \varphi + 2c \cdot \sigma_i \tan \varphi) \\ B = 2c \sin \varphi \cdot \cos \varphi \\ D = \sin^2 \varphi \end{cases} \quad (14)$$

Then formula(13) can be simplified as:

$$\sigma_G = -\sqrt{D \cdot \sigma_i^2 + B \cdot \sigma_i + A} + \sigma_i \quad (15)$$

In the same vein, formula(12) can be simplified as:

$$\sigma_G = -\sqrt{D \cdot \sigma_3^2 + B \cdot \sigma_3 + A} + \sigma_3 \quad (16)$$

Formula(15) and formula(16) are equal:

$$\sqrt{D \cdot \sigma_3^2 + B \cdot \sigma_3 + A} + \sigma_3 = -\sqrt{D \cdot \sigma_i^2 + B \cdot \sigma_i + A} + \sigma_i \quad (17)$$

After transforming formula(17),  $\sigma_3$  can be calculated as follows:

$$\sigma_3 = \frac{-\sqrt{4 \cos^2 \varphi (2 \sigma_i \sqrt{D \cdot \sigma_i^2 + B \cdot \sigma_i + A} - D \cdot \sigma_i^2 - B \cdot \sigma_i - \sigma_i^2) + (2 \sigma_i + B - 2 \sqrt{D \cdot \sigma_i^2 + B \cdot \sigma_i + A})^2}}{2 \cos^2 \varphi} + \frac{2 \sigma_i + B - 2 \sqrt{D \cdot \sigma_i^2 + B \cdot \sigma_i + A}}{2 \cos^2 \varphi} \quad (18)$$

When the soil is in an active limit equilibrium state,  $\sigma_1 = \gamma z$ , and  $\sigma_3 = p_a$ . Then it can be inferred from formula(18) that:

$$p_a = \frac{-\sqrt{4 \cos^2 \varphi (2 \gamma z \sqrt{D (\gamma z)^2 + B \gamma z + A} - D \cdot (\gamma z)^2 - B \cdot \gamma z - (\gamma z)^2) + (2 \gamma z + B - 2 \sqrt{D (\gamma z)^2 + B \cdot \gamma z + A})^2}}{2 \cos^2 \varphi} + \frac{2 \gamma z + B - 2 \sqrt{D (\gamma z)^2 + B \cdot \gamma z + A}}{2 \cos^2 \varphi} \quad (19)$$

where  $\gamma$  refers to the weight of the backfill behind the wall, and  $z$  refers to the depth of the backfill behind the wall.

### (3) Verification of the new method of calculating active earth pressures

To verify the joint strength method, active earth pressures on a retaining wall (Fig.3) at the height of 25m are calculated. The calculation conditions are as follows:

In condition C1-1: cohesive force  $c=20\text{kPa}$ , internal friction angle  $\varphi=20^\circ$ , and tensile strength  $\sigma_t$  of soil  $=-12\text{kPa}$ .

In condition C1-2: cohesive force  $c=40\text{kPa}$ , internal friction angle  $\varphi=20^\circ$ , and tensile strength  $\sigma_t$  of soil  $=-25\text{kPa}$ .

In condition C1-3: cohesive force  $c=60\text{kPa}$ , internal friction angle  $\varphi=20^\circ$ , and tensile strength  $\sigma_t$  of soil  $=-37\text{kPa}$ .

After putting the parameters into formula(3) and formula(19), two distribution curves can be obtained, as shown in Fig. 6.

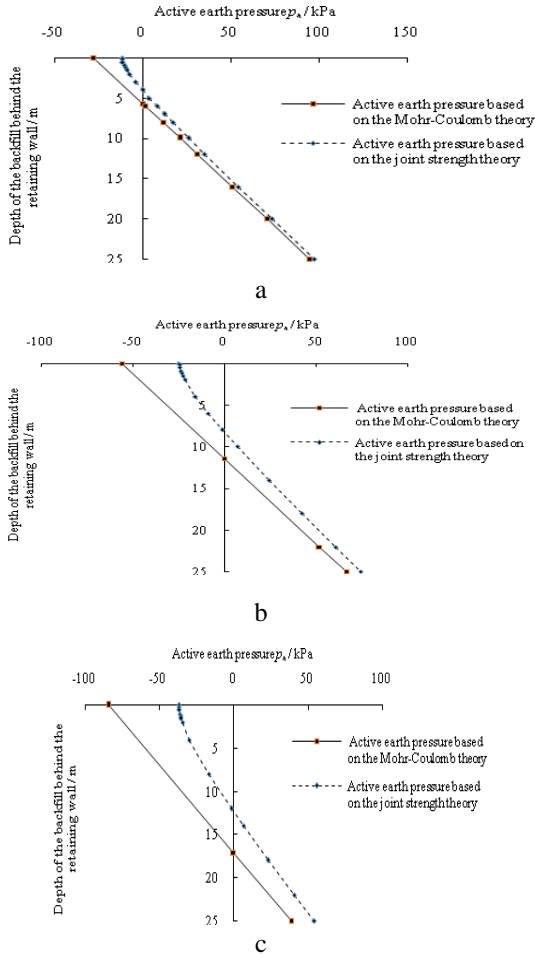


**Fig. 6.** The distribution curves of active earth pressure: (a) Calculation condition C1-1; (b) Calculation condition C1-2; (c) Calculation condition C1-3

It can be known from Fig.6: active earth pressure values of loess based on the joint strength theory are nonlinearly distributed and larger than Rankine’s active earth pressure values; the tensile crack depth of the backfill behind the wall based on the joint strength theory is smaller than that based on the Mohr-Coulomb theory.

The above results show that the Mohr-Coulomb strength theory overestimates the tensile strength of loess.

### Derivation and analysis of passive earth pressures of loess based on the joint strength theory

#### (1) Analysis of limit equilibrium state in passive earth pressure

When the horizontal force  $\sigma_h$  increases to a certain extent, the Mohr’s stress circle is right tangent to the strength line. At this point, the horizontal force  $\sigma_h$  is the passive earth pressure  $p_p$ . The passive limit equilibrium state of soil can be analyzed in two cases (Fig.4). In the first case, the horizontal stress increases to the extent that the

Mohr’s circle is tangent to section II; in the second case, the horizontal stress increases to the extent that the Mohr’s circle is tangent to section III. When the soil is in a state corresponding to the second case:

$$p_p = \gamma z \tan^2 \left( 45^\circ + \frac{\varphi}{2} \right) + 2c \tan \left( 45^\circ + \frac{\varphi}{2} \right) \quad (20)$$

When the soil is in a state corresponding to the first case, passive earth pressures of loess can be derived based on the joint strength.

#### (2) Derivation of new loess passive earth pressure

When the Mohr’s stress circle is in a passive limit equilibrium state (Fig.7). Assume that point N is the tangent point, point M is the center of the Mohr’s stress circle, and line segment NQ is perpendicular to axis  $\sigma$  with point Q as the pedal point.

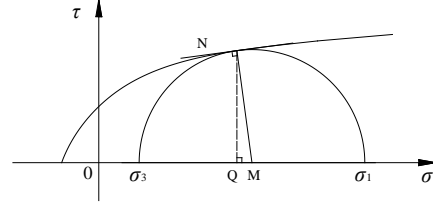


**Fig. 7.** The passive limit equilibrium state.

According to the method of Section 3.1.2. It can be inferred that:

$$\sigma_N = \sqrt{D \cdot \sigma_1^2 + B \cdot \sigma_1 + A} + \sigma_1 \quad (21)$$

$$\sigma_N = \sqrt{D \cdot \sigma_3^2 + B \cdot \sigma_3 + A} + \sigma_3 \quad (22)$$

Formula(21) and formula(22) are equal. After transforming formula,  $\sigma_1$  can be calculated, and  $\sigma_3 = \gamma z$ , and  $\sigma_1 = p_p$ , therefore:

$$p_p = \frac{\sqrt{-4 \cos^2 \varphi (2\gamma z \sqrt{D(\gamma z)^2 + B\gamma z + A} + D \cdot (\gamma z)^2 + B \cdot \gamma z + (\gamma z)^2) + (2\gamma z + B + 2\sqrt{D(\gamma z)^2 + B \cdot \gamma z + A})^2}}{2 \cos^2 \varphi} + \frac{2\gamma z + B + 2\sqrt{D \cdot (\gamma z)^2 + B \cdot \gamma z + A}}{2 \cos^2 \varphi} \quad (23)$$

#### (3) Calculating verification of passive earth pressures

To verify the joint strength theory, passive earth pressures on a retaining wall (Fig.3) at the height of 25m are calculated and analyzed. The adopted groups of parameters are identical to those in Section 3.1.3.

After putting these different condition parameters into formula(20) and formula(23) respectively, two distribution curves of passive earth pressures can be obtained, as shown in Fig.8.

It can be obtained from Figure 8: passive earth pressure values of loess based on the joint strength theory are approximately linear distribution and smaller than Rankine’s passive earth pressure values; with increasing backfill depths, passive earth

pressure values of loess based on the joint strength theory and Rankine's passive earth pressure values gradually approach.

The above results show that the Mohr-Coulomb strength theory overestimates the tensile strength of loess.

and passive earth pressures of loess can be reasonably evaluated by the joint strength theory.

**Acknowledgments:** This research was supported by the NSFC (41472296), China Geological Survey Project (DD20160271) and Scientific Research Program of Shaanxi Provincial Education Department (14JS064). The authors' special appreciation goes to the reviewers of this manuscript for their useful comments.

### REFERENCES

1. R. Nova, L. Gabrieli, Soil Mechanics, Wiley-Iste, American, 2010.
2. C.A. Coulomb, Essais sur une application des regles des maximis et minimis a quelques problems de statique relatifs a l'architecture. Mem. Acad. Roy. Pres. Drivers, save, Paris, 1776.
3. W.J.M. Rankine, *Philosophical Transactions of the Royal Society of London*, **147**, 9 (1857).
4. Q.-D. Xie, J. He, J. Liu, J.-Y. Youyang, *Chinese Journal of Geotechnical Engineering*, **25**, 343 (2003).
5. J.-P. Gao, Y.-L. Liu, M.-H. Yu, *Journal of Xi'an Jiaotong University*, **40**, 357 (2006).
6. J. Zhang, R.-L. Hu, H.-B. Liu, S.-S. Wang, *Chinese Journal of Rock Mechanics and Engineering*, **29**, 3169 (2010).
7. T. Nakai, *Soils and Foundations*, **3**, 99 (1985).
8. J.-M. Zhu, Q. Zhao, *Rock and Soil Mechanics*, **35**, 2501 (2014).
9. J.-Q. Hu, Y.-H. Zhang, L. Chen, J.-G. Chen, *Chinese Journal of Geotechnical Engineering*, **35**, 381 (2013).
10. J.-H. Zhao, W.-B. Liang Wen, C. G. Zhang, Y. Li, *Rock and Soil Mechanics*, **34**, 609 (2013).
11. L. Ma, S.-J. Shao, C.-L. Chen, *Chinese Journal of Underground Space and Engineering*, **9**, 596 (2013).
12. R.-J. Li, J.-D. Liu, R. Yan, W. Zheng, S.-J. Shao, *Water Science and Engineering*, **7**, 319 (2014).
13. R.-J. Li, J.-D. Liu, R. Yan, W. Zheng, S.-J. Shao, *Disaster Advances*, **6**, 316 (2013).
14. R.-J. Li, J.-D. Liu, W. Zheng, R. Yan, S.-J. Shao, *Chinese Journal of Geotechnical Engineering*, **35**, 247 (2013).
15. Y.-X. Song, R.-J. Li, J.-D. Liu, H.-Y. Gao, *Rock and Soil Mechanics*, **35**(6), 1534 (2014).

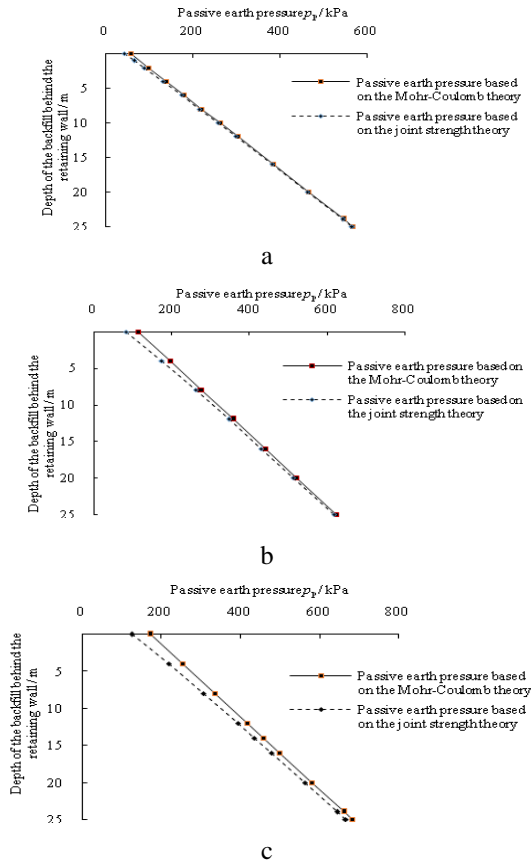


**Fig. 8.** The distribution curves of passive earth pressures: (a) Calculation condition C2-1; (b) Calculation condition C2-2; (c) Calculation condition C2-3.

### DISCUSSION

The Mohr-Coulomb strength theory overestimates the tensile strength of loess, ultimately leading to small Rankine's active earth pressures and large Rankine's passive earth pressures in the calculation. In contrast, due to the proper consideration of the tensile strength of loess, active